



---

# THE ASSESMENT OF PILE SHAFT RESISTANCE BASED ON AXIAL STRAIN MEASUREMENTS DURING THE LOADING TEST

---

ANDREJ ŠTRUKELJ, STANISLAV ŠKRABL, KSENIJA ŠTERN and JANKO LOGAR

---

## about the authors

Andrej Štrukelj  
University of Maribor,  
Faculty of Civil Engineering  
Smetanova ulica 17, 2000 Maribor, Slovenia  
E-mail: andrej.strukelj@uni-mb.si

Stanislav Škrabl  
University of Maribor,  
Faculty of Civil Engineering  
Smetanova ulica 17, 2000 Maribor, Slovenija  
E-mail: stanislav.skrabl@uni-mb.si

Ksenija Štern  
Geoinženiring Ltd.  
Gorkega ulica 1, 2000 Maribor, Slovenija  
E-mail: geoinzeniring.mb@amis.net

Janko Logar  
University of Ljubljana,  
Faculty of Civil Engineering and Geodesy  
Jamova 2, 1000 Ljubljana, Slovenija  
E-mail: jlogar@fgg.uni-lj.si

---

## abstract

*Near Maribor, a new bridge over the Drava river is being under construction. Before the main works actually started, static and dynamic loading tests of piles were performed. The goal of the static loading test was to determine the bearing capacity of the test pile. It was also interesting to determine the share of the axial load distributed on the shaft and pile toe. In order to measure the distribution of the axial force along the pile, a specially made steel canal was built in the pile before concreting. Inside this canal the strain gauges were distributed evenly at the distance of one meter. The strains were measured for each loading phase in all measuring points. The distribution of the axial force was assessed from the obtained results and based on the distribution of the axial force the shaft resistance could be determined. The unexpectedly high bearing capacity of the pile shaft made the obtained results highly interesting. In this paper, measuring methods and measuring results are discussed. Behaviour of the pile*

*and the soil during the loading test were also modelled by axial symmetric and three dimensional models. The calculated and measured results show a very good agreement.*

---

## keywords

pile shaft resistance, loading test, strain measurements, elasto-plastic modelling, Finite Elements Method

---

## 1 INTRODUCTION

According to [1] there are two ways to perform static loading tests of piles. In the first case, the testing pile is loaded by the ballast weight distributed over the special structure made of steel beams on the top of the testing pile. This method is very expensive because of high transportation and manipulation costs of the ballast. More suitable is the second way which requires additional reaction or anchor piles positioned around the testing pile. The distances between the testing pile and anchor piles should be at least three diameters of a pile or 2.5 m (suggestion of the German Geotechnical Society) to reduce the interaction between the compressed and tensioned piles. All of the anchor piles should be linked by a structure of high stiffness made of reinforced concrete (pile plate) or steel beams to ensure the support of hydraulic jacks used for introducing the loading force to the testing pile.

The case described in this paper further optimizes the idea of performing the static pile loading test with the reaction piles by utilizing the final bridge foundation as a reaction frame for the test pile. One of 18 foundations that will support the bridge over Drava and its channel was performed in advance together with the test pile in the centre as shown in Figs. 4 and 5. Additional test pile was constructed 20 m away and was used for the dynamic loading test.





## 2 DESCRIPTION OF THE TESTING SITE

### 2.1 SITE CONDITIONS

On the location of the test pile the Drava river deposited a 15.5 m thick layer of dense poorly graded silty and sandy gravel GP-GM with boulders over the Miocene base of sandy marl. The marl base is partly weathered and contains thin lenses of fine sand. The silty and sandy gravel were investigated in terms of SPT tests and Ménard pressuremeter tests, whereas the marl base was predominantly tested in laboratory to obtain its unconfined compressive strength.

Ground water level was encountered at 6.5 m below the surface.

The number of blows required to drive the standard split-barrel sampler of 30.5 cm in gravelly soil on the considered location was  $N = 33-73$ . Based on the average blow count obtained in silty gravel the characteristic value of the internal friction angle for the design of foundation was estimated to be  $35^\circ$ . The density index assessed from SPT results varied from 0.55 to 0.85. The unit weight of this layer was  $21 \text{ kN/m}^3$ . The net limit pressure from pressuremeter tests varied from  $p_l = 1600$  to  $3300 \text{ kPa}$  and pressuremeter modulus from 11 to 20 MPa.

In marl, the SPT penetrability tests gave  $P = 4-7 \text{ cm}/60$  blows. The unit weight measured on samples from marl bedrock was  $\gamma = 22.1-23.5 \text{ kN/m}^3$ . From the direct shear tests the results were:  $c = 25-56 \text{ kPa}$ ,  $\varphi = 21-31^\circ$ . The unconfined compressive strength varied considerably

along the 760 m long bridge. On the location of the test pile the lowest  $q_u$  values were obtained ( $q_u = 826 - 1844 \text{ kPa}$  at the depth of pile tip and up to  $4730 \text{ kPa}$  at greater depths). In two boreholes in the vicinity of the test pile, performed for the design of other bridge foundations the results were slightly higher and varied from  $q_u = 1948 - 4287 \text{ kPa}$ . The characteristic value of  $q_u = 1850 \text{ kPa}$  was used for the foundation design. Such a low strength value for the bedrock led to expensive foundation design in the preliminary design stage. For this reason the reliability of reported UCS values was put under question.

The load tests on test piles were then suggested to measure pile behaviour subjected to axial loading reliably on site and to verify design proposals.

### 2.2 TEST PILE ARRANGEMENT

On the location of the test pile the support of the future bridge over the river Drava was designed on six piles of  $\phi 150 \text{ cm}$ . These six piles together with the pile plate of 2.0 m thickness were used as the anchoring construction for the test pile of  $\phi 80 \text{ cm}$  diameter situated in the centre of the group of the anchoring piles (Fig. 5). The micro location of the area where the pile testing was performed has been carefully chosen as the machines had unlimited access (Fig. 1). In accordance with the proposed program the depth of the excavation for the testing pile was 17.80 m below the initial surface. The final length of the testing pile together with the widening on the top was 14.70 m. The length of the underground part of the pile was 13.50 m. As the thickness of the sand and gravel layer was about 11.50 m, the testing pile was embedded for about 2.0 m into the marl base (Fig. 4).



Figure 1. Testing site.



### 3 THE PREPARATION OF MEASUREMENT POINTS AND TECHNOLOGY OF MEASUREMENTS

Relative displacements of the pile head with regard to the lower side of the pile plate were registered as the extension of the cylinder of each hydraulic jack which was measured using the special inductive displacement transducers. The same results were obtained by the two



Figure 2. Hydraulic jacks and measurement equipment in the beginning of loading test.

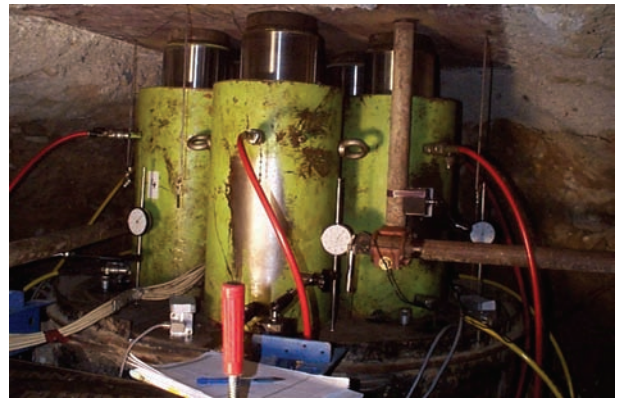


Figure 3. Hydraulic jacks and measurement equipment at the end of loading test.

inductive displacement transducers fixed to the lower side of the pile plate and pointed to the pile head.

Absolute displacements were obtained by dial gages positioned on the stand-alone beam construction. To control the accuracy of all three methods of the pile head settlements measurements the vertical displacements of the pile plate upper surface have been geodetically controlled. The measurement point situated directly above the testing pile has been equipped with the special

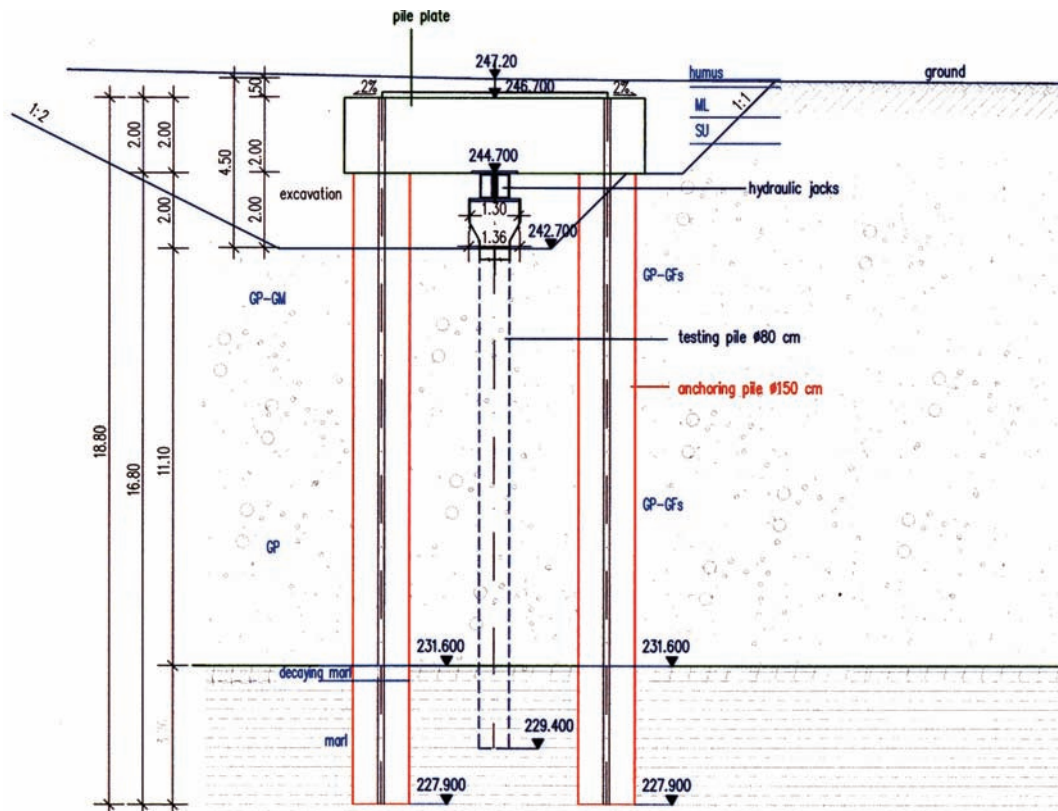


Figure 4. The cross section of the testing site

leveling staff with a bar code compatible with the automatic digital leveler. To ensure the absolute immovability of the instrument base, the steel plate, where the leveler had been fixed, was fixed on the head of the pile which was located 20 m away from the measured pile prepared for the dynamical testing performed later. The precision of the measuring results was  $\pm 0.02$  mm. The vertical displacements above the six anchor piles have been measured using the total station. To make this possible, the six measurement points had to be equipped with the reflexive geodetic targets. The maximally measured displacement above the testing pile was 1.10 mm and the maximally measured displacement above the anchor piles was 0.50 mm. All of the vertical displacements of the pile plate were elastic and after unloading no residual deformations were detected.

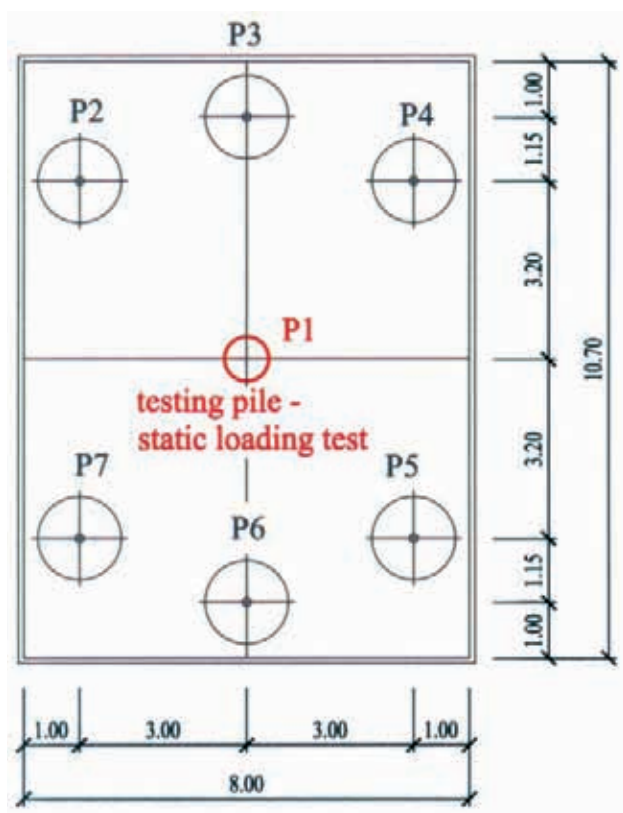


Figure 5. The plan view of the testing site.

#### 4 MEASUREMENTS OF STRAINS ALONG THE PILE AXIS

The most interesting part of the test was to measure the normal strains of the pile in its axial direction in measuring points distributed in equal distances along the pile axis. These strains are proportional to axial forces in the pile. When the course of the axial force

along the pile axis is known, the resistance of the pile shaft can be estimated.



Figure 6. Preparing of measuring channels.

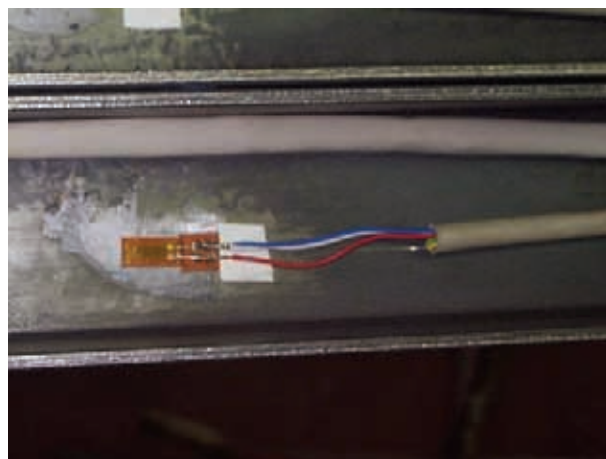


Figure 7. A strain gauge applied inside the measuring channel.

Each measuring point was equipped with two strain gauges (the main one and the spare one). They were distributed in equal distances of 1.0 m starting 0.5 m above the pile toe. As the strain gauges, electrical contacts and communication cables are very sensitive, the moisture and mechanical burdening could be very harmful. So the measuring points were protected with special care. To insure the mechanical protection of the chain of strain gauges together with the communication cables the whole measuring system was built inside the steel channel made of two standard C-profiles (Figs. 6 and 7). The interior surface of the steel channel also served as the ground surface for the strain gauges to be glued on. From transportation reasons the channel was made from three segments that could be easily put together. The mutual connection of the segments was ensured by a special system of joints. The outside channel surface was degreased and made rough to

ensure the adhesion with concrete. Each strain gauge inside the channel was protected against moisture by two layers of putty resistant even under water. When the measuring channel was finished it was connected to the pile reinforcement and put into the pit prepared for pile concreting (Figs. 8 and 9). During the loading test, the communication cables were connected to the Data acquisition unit which was connected to a personal computer. The sampling frequency was 0.2 Hz during the entire measuring period.



Figure 8. The measurement channel fixed between the reinforcement of the pile.



Figure 9. The reinforcement of the pile and the measurement channel during placement into the final position.

## 5 THE METHODOLOGY OF LOADING

The expected limit load (11,9 MN) of the test pile was applied in seven steps of 1700 kN using five synchro-

nized hydraulic jacks. During each loading step the settlements were observed for 60 minutes. As the settlements after 60 minutes did not calm down, the last two loading steps were observed for 120 and 90 minutes.

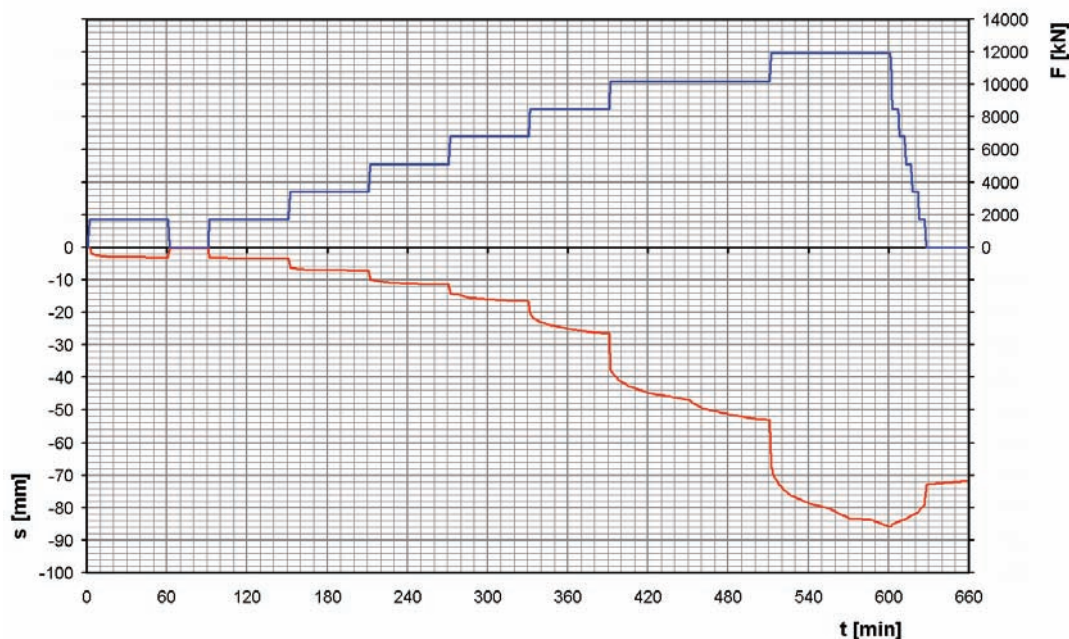


Figure 10. The time history of loading ( $F$ ) and vertical displacements ( $s$ ) of the tested pile.

## 6 MEASUREMENT RESULTS

Axial strains along the pile axis were measured in the measurement points distributed evenly along the measurement channel at the distances of 1.0 m. Because of the settlements of the pile, the loading forces could not be perfectly constant during the periods of individual loading phases. So the electronic control of the hydraulic pump was used to balance the loading forces to the programmed level.

All of the loading phases and even the effects of the loading force corrections during the test can be clearly seen in Fig. 11, where the time history of the strains in all measurement points is shown. The values shown in the

Legend (0.5 m, 1.5 m, ...) represent the distances of the individual measurement points from the pile toe. The obtained results can be interpreted also in other ways. In Fig. 12 the loading stages are marked with 1, 2, 3, 4, 5, 6 and 7, whereas the phase 1a represents the unloading after the first loading step. Other numbers represent other loading stages.

In Fig. 12 the portions of the pile axial load for all above stated loading steps are shown. The values are calculated as the percentage of measured strains regarding the measured strain in the highest measuring point directly below the top of the pile where hydraulic jacks were placed. It can be seen from Fig. 12 that the maximum percentage of the pile toe loading is about 20 %. This value was reached during the final loading stage.

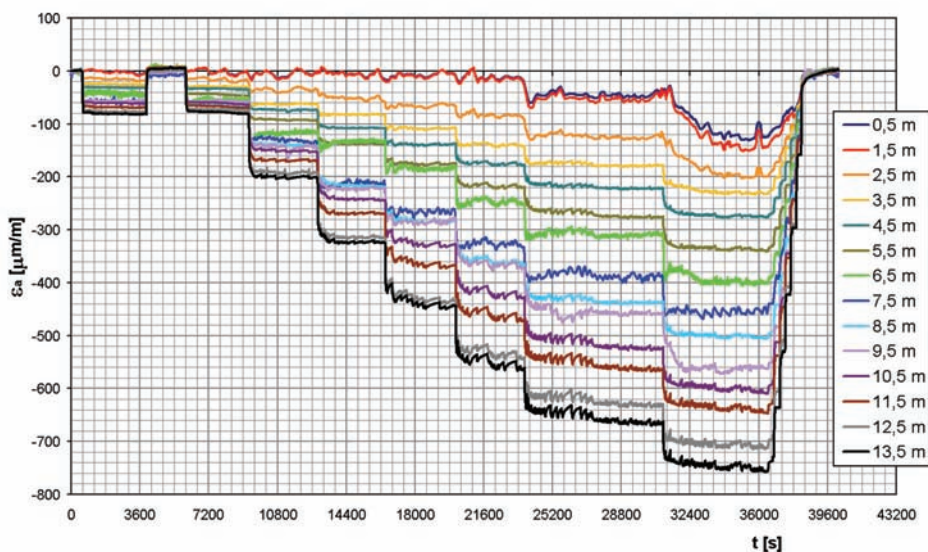


Figure 11. The time history of the normal strains ( $\epsilon_a$ ) of the pile in its axial direction.

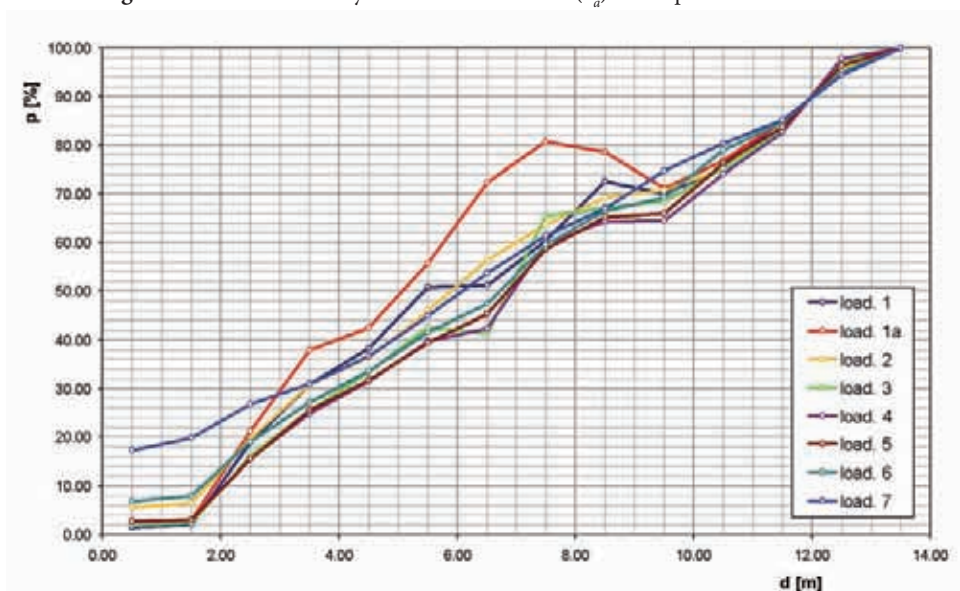


Figure 12. The portion of the pile axial load ( $p$ ) for all loading phases versus the distance from the pile toe ( $d$ ).

The normal stresses in axial direction for all loading phases were calculated considering the average value of the elastic modulus of concrete of 30.0 GPa. If these values are multiplied by the value of the pile cross-section, a very good estimation can be obtained for the axial force of the pile (Fig. 13). As the values of the axial force at the highest measurement point coincide with the values of the loading force applied to the pile head, the correctness of the measured results is additionally proved.

It can also be seen from Figure 13 that the bearing capacity below the pile toe was first activated not earlier than at the last but one loading stage (10200 kN). During the last loading stage the increment of the loading force was 1700 kN and the increment of the activated axial force in the pile toe was 1300 kN. Therefore, even at the last loading phase the small part of the loading force was taken by the pile shaft.

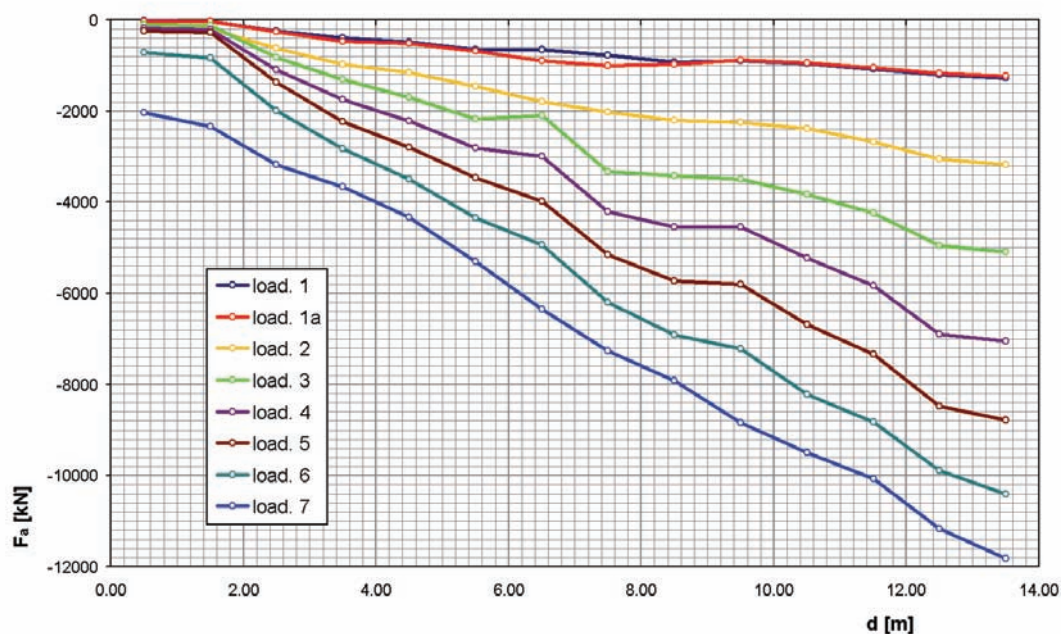


Figure 13. The axial forces ( $F_a$ ) of the pile versus the distance ( $d$ ) from the pile toe.

The measured load settlement curve for the pile top is presented in Fig. 17 together with the results of numerical modelling. This curve shows the considerable increase of settlement in the last two loading stages. In the last loading stage the pile settled for over 80 mm which is more than 10% of the pile diameter. The load of 11,9 MN can therefore be considered as ultimate bearing capacity of the test pile according to the Eurocode 7-1.

## 7 THE ANALYSIS OF THE MEASUREMENT RESULTS

The measurements of normal strains along the pile axis greatly contributed to the results of the loading test. Since these results are available the analysis of the shear resistance along the pile shaft can be done. It can be seen, that shaft resistance increases linearly up to the loading stage 6. During the last loading stage (loading stage 7) the increment of the shaft resistance is minimal. It can be considered that in the last loading stage the bearing capacity of the pile shaft was fully mobilized (Fig. 14).

The results of the loading test showed that the calculated value for the pile shaft bearing capacity was underestimated. One of the possible reasons for this phenomenon can be the fact that during concreting the concrete pene-

trated into the porous gravel surrounding the pile. The consumption of the concrete was namely approximately 10% higher than it was foreseen, which could lead to the average increase in the pile diameter from theoretical 80 cm to 90 cm. Taking the higher number into account the estimated 300 kPa of average ultimate shaft resistance drops to 265 kPa which is still a high value for the shaft resistance.

On the basis of the static pile loading test it can be considered that until the estimated bearing capacity was reached in the last load step, the whole loading was

taken over exclusively by the pile shaft. It should be emphasized that the limit value of the bearing capacity below the pile toe was not reached. Despite this there was no need for increasing the pile loading since the achieved value of the pile settlement exceeded 10% and was far larger than it is allowed as the future bridge support and the soil around the pile showed distinctive non-linear behaviour. The results of the investigation confirmed the known fact that the bearing capacity of the pile toe can be activated only after relatively high values of pile settlements. On the other hand, the essentially lower values are needed for the activation of the friction along the pile shaft.

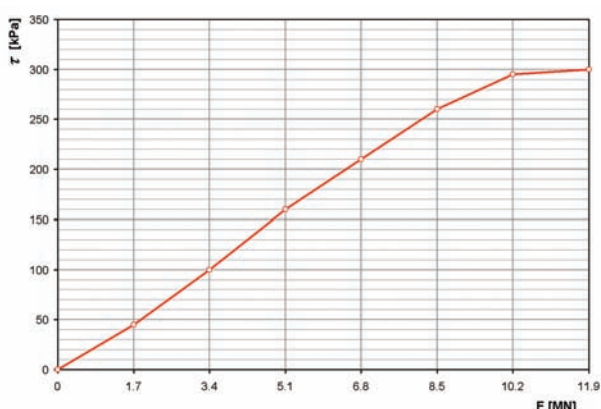


Figure 14. The average pile shaft resistance ( $\tau$ ) as a function on the vertical loading ( $F$ ).

## 8 FINITE ELEMENT ANALYSIS

The results of experimental investigations were confirmed by a set of numerical analyses using the finite element method (FEM). Three and two-dimensional analyses of interaction between a bored reinforced pile loaded with vertical loading and ground were performed for this purpose.

The analyses consider a 13.1 m long pile that is placed in length of 11.2 m in sandy gravel soil GP-GM with boulders and at the depth between 11.2 and 13.3 m in marl base. The ground water level is 6.5 m under the ground level.

Reinforced concrete of pile was considered to be linear elastic with the Young modulus  $E = 30.0$  GPa, Poisson's ratio  $\nu = 0.2$  and unit weight  $\gamma = 25$  kN/m<sup>3</sup>.

Geomechanical properties of the upper sandy gravel layer were determined on the basis of standard penetration test results. This material was modelled in numerical analyses by Hardening-Soil model with isotropic hardening (PLAXIS 1998). This model considers hyper-

bolic dependence between stresses and strains, it enables the consideration of increasing soil stiffness as a function of ground stresses, dilatation and cap yield surface.

In the considered case the most important is dilatation which cannot be incorporated into the Mohr-Coulomb model because of volume changes due to successive pile loading during test performance.

Numerical analyses consider the following material parameters:  $\varphi = 42^\circ$ ,  $\psi = 12^\circ$ ,  $E_{50}^{ref} = E_{oed}^{ref} = 50$  MPa,  $E_{uer}^{ref} = 3 \cdot E_{50}^{ref}$ ,  $\nu_{ur} = 0.2$ ,  $m = 0.5$ ,  $R_f = 0.9$ ,  $e_{in} = 0.5$ ,  $e_{min} = 0.48$ ,  $e_{max} = 0.52$ ,  $\gamma = 21$  kN/m<sup>3</sup> in  $p_{ref} = 1$  MPa.

Marl was modelled as Mohr-Coulomb material model with the following parameters: shear angle  $\varphi = 28^\circ$ , cohesion  $c = 40$  kPa, dilatation  $\psi = 0^\circ$ , Young modulus  $E = 100$  MPa, Poisson's ratio  $\nu = 0.25$  and unit weight  $\gamma = 23$  kN/m<sup>3</sup>.

The test pile of diameter  $D = 0.8$  m was surrounded by six bored cast-in-place piles of diameter  $D = 1.5$  m each. Therefore, in analyses of axis-symmetrical elasto-plastic model, radial movements of the ground were prevented in the radial distance of 5.0 m as a consequence of stiffness due to erection of large diameter piles.

Because of the material losses during pile concreting, which amounted to about 10% of the required concrete mass, a pile of enlarged cross-section, of the diameter of 90 cm was considered in sandy gravel material. This enlargement approximately illustrates the influence of concrete mass penetration into porous sandy gravel material.

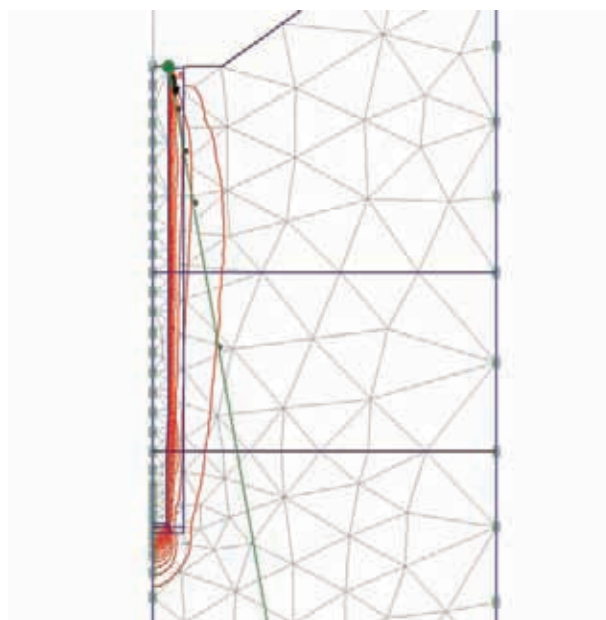


Figure 15. Cross-section of the analysed axis-symmetrical model and distribution of vertical movements in ground (distance of isolines is 5 mm).



The cross-section of the analysed model with finite element mesh and distribution of vertical movements in ground at movement of the top of the pile for 10 cm is presented in Fig. 15.

The analysis of three-dimensional (3D) model (Fig. 16) was performed using the same material parameters as in 2D analysis.

The results of numerical analyses show that the results of axis-symmetrical and 3D model considering pile-bearing capacity at 10 cm of vertical movement do not differ essentially.

Fig. 17 shows the relation between vertical loading and movements of the pile top obtained with the analysis on axis-symmetrical model compared to the measured values.

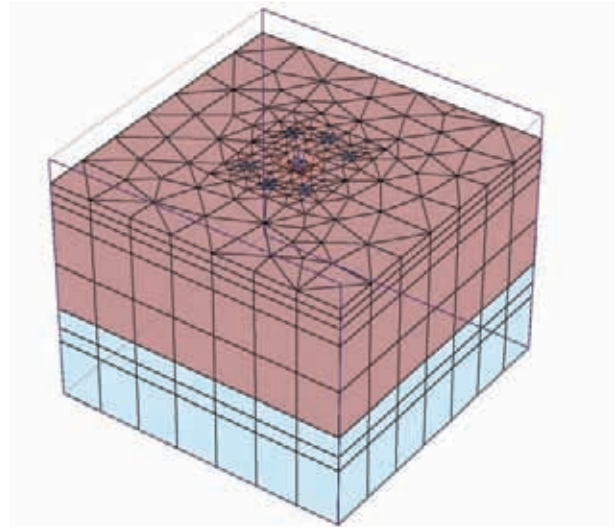


Figure 16. View on 3D elasto-plastic model.

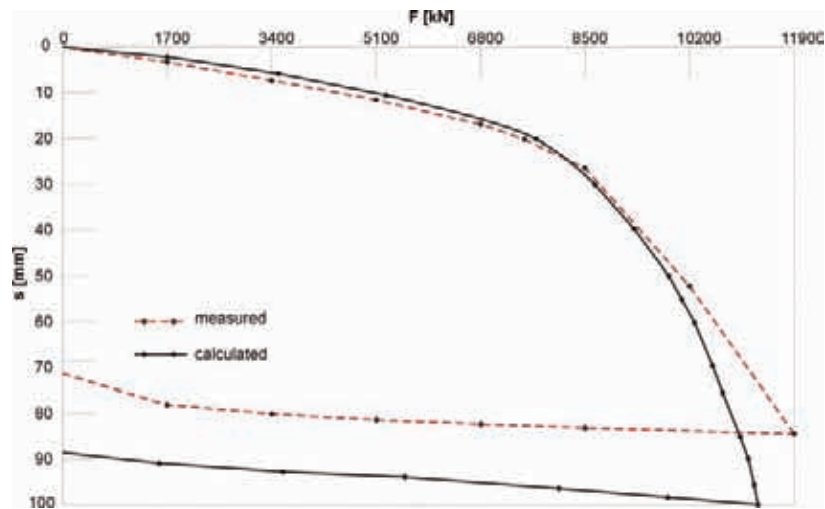


Figure 17. Comparison of calculated and measured values of vertical load ( $F$ ) versus settlement ( $s$ ).

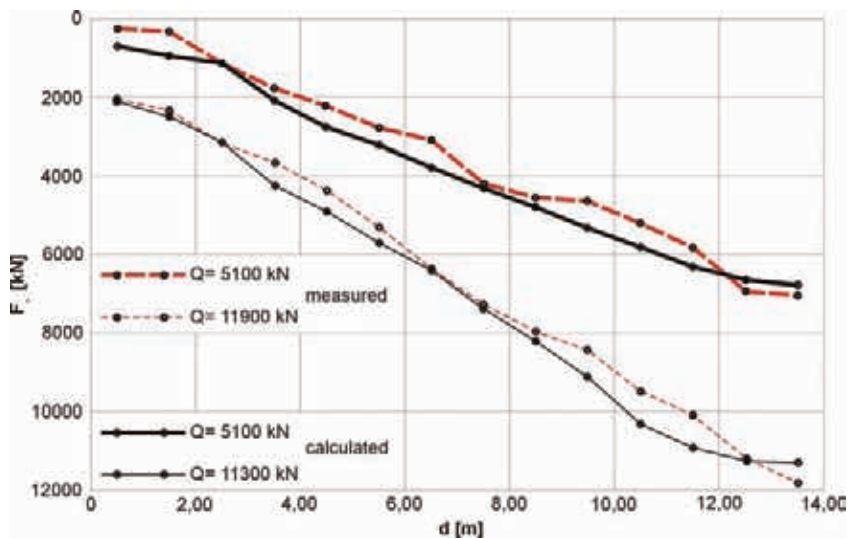


Figure 18. Comparison of calculated and measured values for distribution of axial load ( $F_z$ ) along the pile axis versus distance from the pile toe ( $d$ ).



Fig. 18 presents distribution of axial forces along the pile axis for cases of vertical loading of 5100 kN, the highest numerical analysis value 11300 kN, and the highest test value of 11900 kN, where failure has already occurred and the measurements of settlements could not be taken.

## 9 CONCLUSIONS

The measurement control of geotechnical structures is very important and gives the opportunity to examine the quality of the soil as well as the structures themselves. On the basis of such investigations very useful information can be obtained. The static loading test described above was a good example for such consideration. The precisely and systematically obtained and carefully analyzed measurement results will be an important contribution to the reliability of the foundation design of the future bridge. For the first time the pile static loading test was performed in Slovenia in such a way that instead of ballast, the force of hydraulic jacks against the anchored reacting frame was used to introduce the axial compressive load into the testing pile. As for the anchoring structure, the real bridge support was used, which represents another rationalization and simplification of the testing procedure. This kind of realization proved itself very simple, rational and technically appropriate.

The results of numerical analysis show that anchoring piles of diameter  $\phi = 150$  cm positioned at the distance of 4.2 m do not essentially influence the bearing capacity of a testing pile. Relatively high friction between the tested pile shaft and soil is the result of concrete penetration into sandy gravel soils and dilatation of this material when increasing shear stress on the shaft. If we consider enlarged pile diameter and limited dilatation, the results of FEM analyses agree very well with the results of experimental measurements.

The highest loading obtained with numerical analysis was  $Q = 11300$  kN at vertical movement 10 cm, which is smaller than the measured value  $Q = 11900$  kN. Failure occurred in test and measuring equipment did not allow further measurements of the pile top vertical movement.

We believe that elasto-plastic modelling with FEM and a reasonable use of the Hardening Soil elasto-plastic model of the ground enable to determine the relations between movements and loadings of vertically loaded bored piles to the acceptable accuracy.

Material data used in analysis are valid only for analysing pile bearing capacity in similar geotechnical conditions.

## REFERENCES

- [1] ASTM (1981). *Standard Method for Testing Piles Under Static Axial Compressive Load, Designation: D1143-81*. Philadelphia.
- [2] BOWLES J.E. (1996). *Foundation analysis and design*. McGraw-Hill, New York.
- [3] BRINKGRAVE R.B.J., VERMEER P.A. (1998). *Plaxis, users manual, version 7*. A.A. Balkema, Rotterdam, The Netherlands.
- [4] HOFFMANN K. (1989). *An Introduction to Measurements using Strain Gages*. Hottinger Baldwin Messtechnik GmbH, Darmstadt.
- [5] HOFFMANN K. (1996). *Hinweise zum Applizieren von Dehnungsmessstreifen (DMS), 4. erweiterte Fassung*. Hottinger Baldwin Messtechnik GmbH, Darmstadt.
- [6] ŠTERN K. (2000). *Geološko-tehnično poročilo, AC Koper - Lendava, Most čez Dravo 10-3, 6-1, , arhiv. št. 50-53a/99*. Geoinženiring d.o.o., Ljubljana.
- [7] ŠTERN K., ŠTRUKELJ A. (2001). *Poročilo o rezultatih obremenilnih preizkusov testnih pilotov v podpori 3D mostu čez Kanal in Dravo na AC Slivnica - Pesnica, opr.št. 50-8/2001*. Geoinženiring d.o.o., Ljubljana.

## APPENDIX: NOTATION

The following symbols are used in this paper:

- $c$  = cohesion of the soil,
- $D$  = pile diameter;
- $E$  = module of elasticity;
- $e_{in}$  = initial void ratio of the soil;
- $e_{max}, e_{min}$  = void ratio of the soil in the loosest densest states;
- $E_{50}^{ref}$  = secant stiffness in standard drained triaxial test at the reference pressure;
- $E_{oed}^{ref}$  = tangent stiffness for primary oedometer loading at the reference pressure;
- $E_{ur}^{ref}$  = unloading / reloading stiffness in Hardening-Soil model (considered  $E_{ur}^{ref} = 3 E_{50}^{ref}$ );
- $m$  = parameter in elasto-plastic Hardening-Soil model (it is the input parameter in the relationship for stress dependent stiffness according to a power law);





- $N$  = standard penetration number (blows per 30.5 cm);
- $P$  = penetrability (cm / 60 blows);
- $p^{ref}$  = reference pressure in elasto-plastic Hardening-Soil model;
- $Q$  = vertical load of pile;
- $q_u$  = unconfined compressive strength;
- $R^f$  = parameter in elasto-plastic Hardening-Soil model that defines failure ratio  $q_f / q_a$  (ultimate deviatoric stress / asymptotic value of the shear strength), is derived from the Mohr-Coulomb failure criterion;
- $\gamma$  = unit weight of the soil;
- $\nu$  = Poisson's ratio
- $\nu_{ur}$  = Poisson's ratio for unloading-reloading in Hardening-Soil model (considered  $\nu_{ur} = 0.2$ );
- $\varphi$  = angle of internal friction of the soil;
- $\psi$  = angle of dilatation of the soil.

